Energy and Power Engineering, 2022, 14, 217-232
https://www.scirp.org/journal/epe
ISSN Online: 1947-3818
ISSN Print: 1949-243X

Heavy Duty Natural Gas Single Cylinder Research Engine Installation, Commissioning, and Baseline Testing

Juan Felipe Rodriguez[1], Hui Xu[2], Greg Hampson[3], Bret Windom[1], Anthony Marchese[1], Daniel B. Olsen[1*]

[1]Colorado State University, Fort Collins, CO, USA
[2]Cummins Inc., Columbus, IN, USA
[3]Woodward Inc., Loveland, CO, USA
Email: *Juan.Felipe.Rodriguez@colostate.edu

How to cite this paper: Rodriguez, J.F., Xu, H., Hampson, G., Windom, B., Marchese, A. and Olsen, D.B. (2022) Heavy Duty Natural Gas Single Cylinder Research Engine Installation, Commissioning, and Baseline Testing. *Energy and Power Engineering*, **14**, 217-232.
https://doi.org/10.4236/epe.2022.146012

Received: April 21, 2022
Accepted: June 25, 2022
Published: June 28, 2022

Abstract

Natural Gas (NG) Internal Combustion Engines (ICE) are a promising alternative to diesel engines for on-road heavy-duty applications to reduce greenhouse gas and harmful pollutant emissions. NG engines have not been widely adopted due to the lower thermal efficiency compared with diesel engine counterparts. To develop the base knowledge required to reach the desired efficiency, a Single Cylinder Engine (SCE) is the most effective platform to acquire reliable and repeatable data. A SCE test cell was developed using a Cummins 15-liter six-cylinder heavy-duty engine block modified to fire one cylinder (2.5-liter displacement). A Woodward Large Engine Control Module (LECM) is integrated to permit implementation of real-time advanced combustion control. Intake and exhaust characteristics, fuel composition, and exhaust gas recirculated substitution rate (EGR) are fully adjustable. A high-speed data acquisition system acquires in-cylinder, intake, and exhaust pressure for combustion analysis. The baseline testing shows reliable and consistent results for engine thermal efficiency, indicated mean effective pressure (IMEP), and coefficient of variance of the IMEP over a wide range of operating conditions while achieving effective control of all engine control and operation variables. This test cell will be used to conduct a research program to develop new and innovative control algorithms and CFD optimized combustion chamber designs, allowing ultra-high efficiency and low emissions for NG ICE heavy-duty on-road applications.

Keywords

Single Cylinder Engine, Heat Release, Heavy Duty, Natural Gas, End Gas Auto-Ignition

1. Introduction

Transportation sector is one of the main contributors of greenhouse emissions to the atmosphere, due to internal combustion engines fuelled with petroleum-based fuels. Diesel fuel is the main source of energy in the heavy-duty transportation sector moving up to 80% of freight use and 28% of all domestic fuel consumed per year [1] [2]. The use of diesel fuel and compression ignition engines is motivated mainly by the lower operating cost, higher fuel efficiency and higher durability than equivalent spark ignited engines [3]. Petroleum based fuels are affected by decreasing in crude oil reserves and the political uncertainty scenarios that affect the final price of the fuel. Given the availability of natural gas within the US with the implementation of hydraulic fracking techniques, natural gas appears as a natural alternative for short-term substitution in traditional CI diesel engines. NG is lower in cost, produces no particulate matter, and is lower in CO_2 emissions due to a lower carbon to hydrogen ratio inherent to fuel composition, mainly methane (CH_4). These conditions also represent a lower cost in after treatment systems to meet emission regulations that also represent lower operative costs for the end user [4] [5].

It is desired to achieve higher overall Brake Thermal Efficiency (BTE) of NG engines as this is the main limiting factor for this type of engine to be a viable alternative to traditional Diesel heavy-duty counterparts. To do so, the combustion control of spark ignited homogeneous NG-Air mixtures must be improved. Knock is one of the main limitations of spark ignition engines to achieve higher efficiency. Another requirement is to improve the capability to operate on variable reactivity fuel. Wide regional variances of fuel reactivity make high performance engines difficult to tune for the national market [6].

The work presented on this paper is part of the U.S. Department of Energy project "Expanding the Knock/Emissions/Misfire Limits for the Realization of Ultra-Low Emissions, High Efficiency Heavy Duty Natural Gas Engines". Under this project, several research phases have been accomplished. This research has defined high percentages of exhaust gas recirculation (EGR) conditions and stoichiometric air/fuel ratio as requirements to achieve the performance desired without heavy knocking conditions. In addition, the rapid compression machine (RCM) and CFR engine were used to characterize the effects of variation in natural gas fuel reactivity [6], chemical mechanism optimization, and computational fluid dynamics (CFD) modeling to optimize combustion chamber design [7] [8] [9]. The phase described in this paper is installation, commissioning, and baseline testing of a heavy-duty single cylinder research engine.

Single cylinder engines (SCE's) have been important research tools to reduce emissions and improve performance and fuel consumption from internal combustion engines. In this case, a production engine was modified to deactivate all but one cylinder. This strategy is less time-consuming and costly, as it enables evaluation of custom modifications at lower cost since design and fabrication of hardware for only one cylinder is required [10].

Research will be carried out to using this platform to achieve the overarching goal to address fundamental limitations to achieving diesel-like efficiencies in heavy duty on-road NG engines. The focus is on the Cummins 15-liter heavy duty engine platform, which has a baseline diesel BTE of 44% at peak torque. This paper presents a detailed description of the design, installation, and commissioning of the SCE and test cell.

2. SCE Test Cell

2.1. Engine

A solid model of the current production ISX15 (15-liter) diesel engine converted into a 2.5-liter single cylinder engine is shown in **Figure 1**. The inline, 6-cylinder X15 engine has bore and stroke dimensions of 137 × 169 mm and total displacement of 15 liters. Hence, the displacement of the single, firing cylinder is 2.5 liters. The engine was designed to allow operation up to 25 bar indicated mean effective pressure (IMEP).

While the crankshaft and connecting rods are standard X15 parts, cylinders one to five are deactivated by replacing the pistons with "dummy pistons", machined with a hole in the middle to reduce/eliminate compression but to match the mass of the #6 piston to maintain the balance of the crankshaft (see **Figure 2**). Cylinder #6 (firing cylinder) has new components developed for this application: piston, ring set, cylinder liner, connecting rod, and bearings. This #6 piston has a specific a Cummins proprietary design for the intended spark ignition operation with a compression ratio of 11.5:1 (**Figure 2**).

Spacers were added in place of the original rocker arms to deactivate cylinders #1 - #5 in order to maintain oil pressure and the original design lubrication conditions (**Figure 3**). For the #6 cylinder the head was machined to accept a sparkplug adaptor in place of the original diesel injector. The cylinder head was also machined to install a cylinder pressure transducer (AVL QC34C), shown in **Figure 4**. This transducer uses a machined adapter, so alternative transducer models may

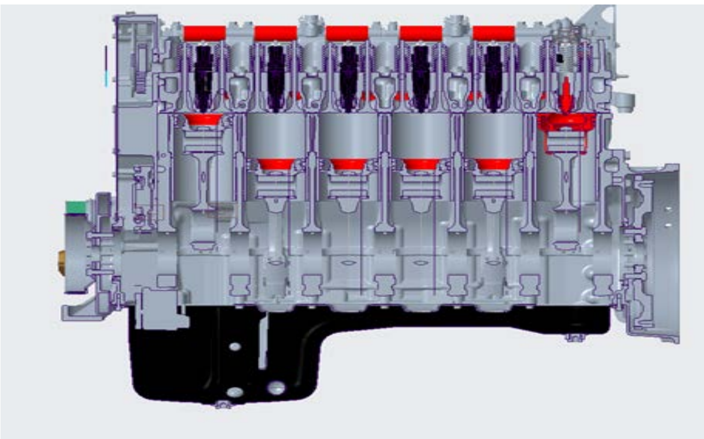

Figure 1. X15 SCE Cummins engine. Deactivated cylinders are #1 to #5, firing cylinder is #6. #5, firing cylinder is #6.

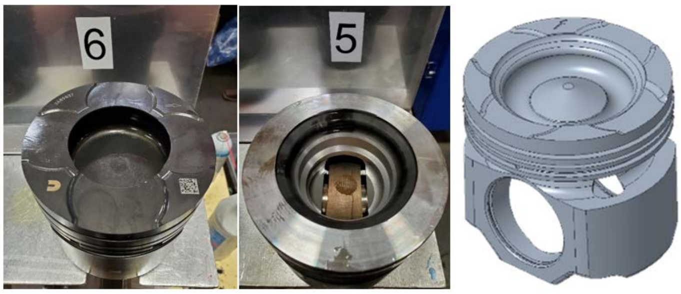

Figure 2. Piston comparison X15 SCE. Right, single cylinder engine spark ignition baseline piston installed in cylinder #6. Center, dummy hollow pistons in cylinders #1 - 5. Right, original diesel X15 piston.

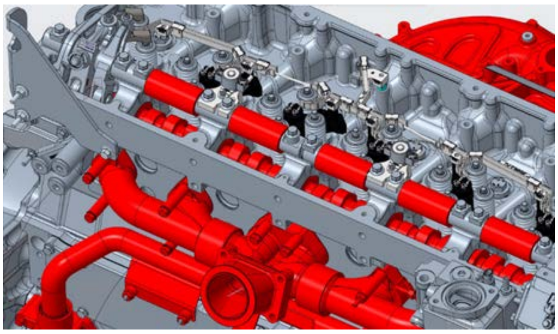

Figure 3. SCE camshaft configuration with rocker arm spacers for cylinders #1 - #5.

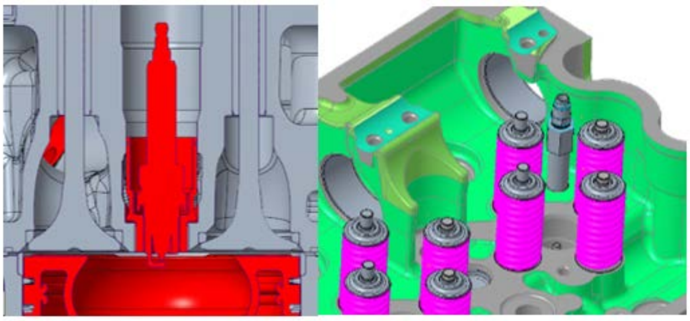

Figure 4. Left, spark plug with spark plug adapter in place of original diesel injector in cylinder #6. Right, pressure sensor installed in cylinder #6 using a machined adapter.

be tested in the future, as installation dimensions are consistent across transducer suppliers.

Additionally, the intake and exhaust manifolds were machined to accommodate high speed Kistler piezo resistive intake (Type 4007D) and water-cooled exhaust (Type 4049B) pressure transducers. These sensors allow for more accurate model validation and tuning 3-D Converge CFD and 1-D GT-Power models of the engine.

In addition to the internal engine modifications previously noted, the following parts were also removed from the original X15 diesel engine:

- Diesel fuel pump, filter, supply lines, high pressure rail system;
- ECU (Engine Control Unit);

- EGR (Exhaust Gas Recirculation) valve and cooler;
- EGR crossover;
- Turbocharger and related parts;
- Engine starter.

2.2. Test Cell

The Cummins X15 SCE test cell is shown in **Figure 5**. The test cell uses an AC electric motor/generator with a regenerative variable frequency drive (VFD) to spin the engine for motored-mode operation and startup and to apply the load. The VFD allows a desired speed to be set and it controls the load to the engine to keep the targeted speed constant or drive the engine if there is no combustion.

The engine is mounted in a specially modified test cell. A steel chassis supports the engine with custom made engine mounts aligning the engine and the motor. Two control panels are located at the sides of the engine and water and air lines run from the facility coolant and compressed air supply systems, respectively.

The engine has its OEM flywheel and uses an adapter plate to connect to the driveshaft. On the other side of the driveshaft, a custom-designed torque tube connects to the electric motor.

The torque tube is a machined hollow aluminum tube with a specific internal and external diameter to deform in a pre-calculated amount while the load is applied. This deformation is measured with strain gauges that feed the signal to the data acquisition system to know the actual torque from the engine.

Cylinder pressure, intake manifold pressure (IMP) and exhaust manifold pressure (EMP) are crank angle synchronized with high-resolution, high-fidelity boundary conditions for combustion analysis. An encoder is connected to the crankshaft, trigger for the data sampling, with 3600 pulses per encoder revolution (7200 per cycle). This encoder is supported in place with a special plate that uses the engine mount as a support and an upper brace to prevent vibrations or deformations that potentially could affect the encoder signal.

Figure 5. Cummins X15 SCE test cell.

The cooling system for the engine is connected to an external water cooling/heating system that allows control of the coolant temperature. This heat exchanger uses water from the facility to allow a continuous operation of the engine without overheating issues. A control valve increases or decreases the cooling water flow as a function of the engine load to maintain optimal engine temperature (85˚C).

The air intake of the engine uses compressed dry air from the air supply of the facility. The intake pressure could be varied up to 60 psi. A Woodward Venturi effect fuel mixer allows the addition of the gaseous fuel to the air supply. The air fuel mixture passes through an intake heater system to simulate the heating from compression from the turbocharging process in a real engine. Following this, there is the addition of the exhaust recirculated gases coming from an in house designed and fabricated EGR cart. This EGR cart, allows to condition the exhaust gases recirculated in temperature and pressure, measure the EGR gas flow and adjust the EGR rate using a VFD, 1hp electric motor and a Speedaire-2EPP4 blower pump that allows EGR substitution rates from 5% to 40%. Finally, a Woodward throttle valve is controlled through the LabVIEW system to regulate the air fuel mixture to the engine. The exhaust system is custom made and allows for emissions, temperature, and pressure sampling. This system also includes an exhaust backpressure valve to simulate the effects of the turbocharger exhaust turbine in a real engine. A port feeds the EGR cart with exhaust gases to be conditioned and recirculated back to the intake system.

A special oil heating system was developed to allow the engine to operate within the design limits for oil temperature while the engine is running with just one cylinder. This system takes oil from the oil pan with a 1 kW pump, and feeds a 6 kW heater array before returning the oil to the engine sump. The nominal oil temperature for this engine is 105˚C.

2.3. Controls

The engine and test cell are controlled through two main modules, Woodward's Large Engine Control Module (LECM), and a National Instruments (NI PXI 1050 chassis with 6224 and 6704 modules) data acquisition and control module. The LECM is a control unit designed to operate reciprocating engines (gas, diesel, or dual fuel) used in power generation, marine propulsion, locomotive and industrial engines, and process markets. This system uses a single-box approach that can be built up with interlocking modules into a single engine-mountable assembly. This control scheme uses a modular approach for both the electronic control modules and software. Each module has its own microprocessor and runs its own software routines, written in Woodward's MotoHawk software, using proven core functions and algorithms. The modules all share their information in a real-time manner, making the entire system act as one fully integrated controller [1]. For this application, the system was configured with an electronic ignition driver module (EID), and auxiliary module for in cylinder pressure analysis and knock detection, and a main module for fuel management. Figure 6 presents the general schematic for LECM control tasks. Fuel flow (equivalence ratio) and ignition timing (combustion phasing) are the two LECM control duties for this application.

The LECM was selected because Woodward has developed efficient and comprehensive cycle resolved combustion diagnostics using high efficiency smart algorithms. Each cycle is analyzed in real-time, including heat release and mass fraction burn calculations. This technology, called Real-Time Combustion Diagnostics and Control (RT-CDC), can be viewed as a Smart Sensor, where key combustion metrics such as IMEP, peak pressure location and magnitude, burn duration (10% - 90%), location of 50% burn duration (CA50), and misfire can be calculated in the time of one engine cycle and put onto the data bus for use by the LECM. The RT-CDC system can monitor the pressure trace and heat release and generate the crank angle at which EGAI occurs and calculate the fraction of end-gas autoignition (f-EGAI, defined earlier). Then C-EGAI is employed to maintain constant f-EGAI for each cycle by modulation of primary parameters such as spark timing, fueling, and EGR rates. As engine operation, fuel quality, and ambient conditions change, the LECM can adapt at least one parameter such as spark timing so that a target f-EGAI is maintained over all engine operating conditions.

The National Instruments based system uses a LabVIEW custom made virtual instrument to control the throttle, air intake pressure and temperature, exhaust back-pressure, EGR ratio and dynamometer. In Figure 7, the black lines show

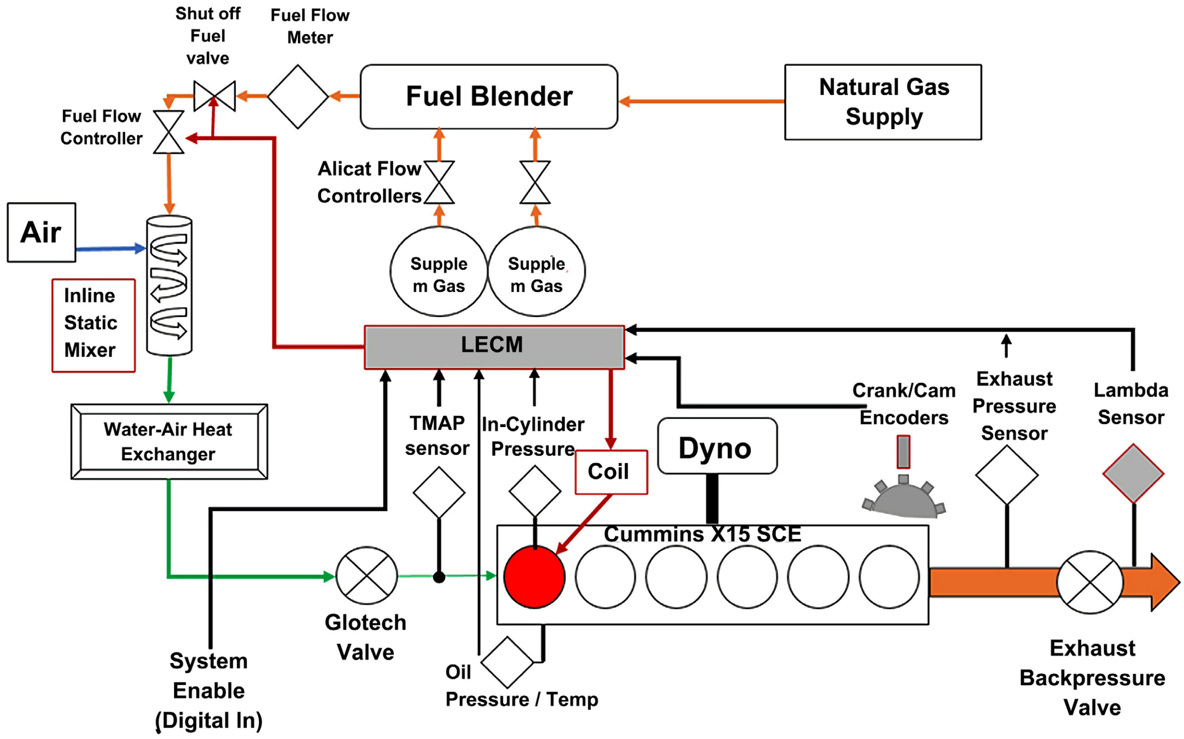

Figure 6. X15 SCE LECM schematic.

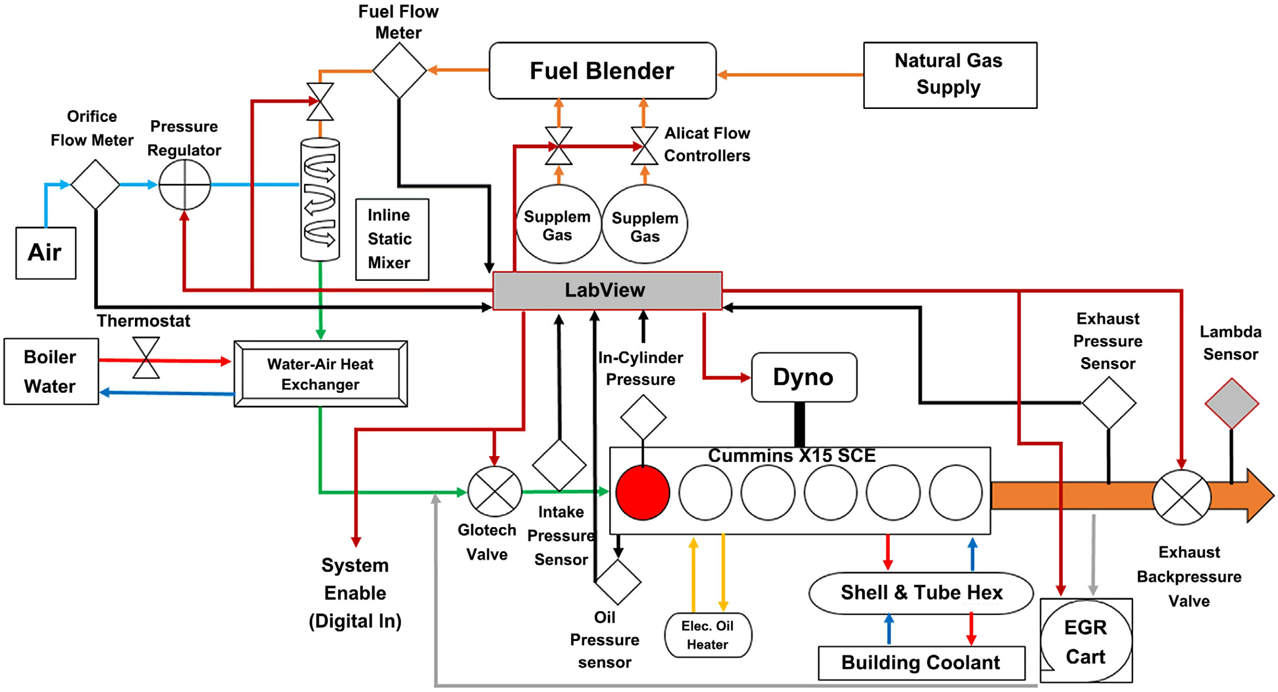

Figure 7. X15 SCE LabVIEW schematic.

which sensors will be feeding the control modules, which will control the actuators (red lines). This system utilizes low speed sampling and controls and monitors overall test cell parameters including temperatures, pressures, and flows, with a sample rate of 2 Hz.

The additional high-speed sampling for the in-cylinder pressure and dynamic intake and exhaust sensors uses a national instruments based high speed system (NI PXIe 1071 chassis with NI PIXe 6363 module) running an in-house developed combustion logger virtual instruments in LabVIEW. This system allows for a 0.1 deg sampling rate (3600 samples per revolution). Performance metrics based on combustion pressure data include IMEP, Peak Pressure coefficient of variation (COV), IMEP COV, CA50, Start of Combustion, Heat Release and Knock Index.

2.4. Emissions Measurement

The exhaust manifold is equipped with an emission sampling port and heated sample line. Exhaust gas concentration measurements for CO, CO_2, NO_x, O_2, and THC from a Siemens 600 series 5-gas Analyzer system (Ultramat, Noxmat, Oxymat and Fidamat respectively) and formaldehyde, speciated hydrocarbons up to C_3, NO, and NO_2 measured with an MKS Multigas 2030 FTIR spectrometer are available during the engine operation. Additionally, fuel composition (CH_4, C_2H_6, C_3H_8, i-C_4H_{10}, n-C_4H_{10}, i-C_5H_{12}, n-C_5H_{12}, n-C_6H_{14}, N_2, CO_2) is analyzed during the operation of the engine with an Variant CP-4900 MicroGC Analyzer.

2.5. Exhaust Gas Recirculated Rate

The exhaust gas recirculation rate was a critical aspect in this research, as is part of the strategies to increase the BTE as consequence of running at higher IMEP. To be a useful tool, recirculated exhaust gases flow measurement must be accurate. To achieve this, a CO_2 concentration analysis was performed, using the concentration of CO_2 in the intake air, fuel, and recirculated exhaust gases, to find the mass flow of EGR and then the equivalent EGR rate. Mass flow of air is quantified from the Coriolis fuel flow measurement and the Air/Fuel ratio measured with a lambda sensor, while molar concentrations of CO_2 in each flow was measured with the 5-gas analyzer. This EGR flow quantification allowed calibration of the orifice plate measurement device on the EGR cart to simplify the measurement process during testing. The calibration data is presented in Figure 8. EGR rate quantification requires gas composition measurement of the exhaust gases and the intake mixture of gases on the intake (Air + Fuel + EGR). Fuel composition is obtained from the GC fuel analyzer. Composition measurement for each mixture is used to determine the molar mass knowing pressure and temperature conditions of fuel line at the GC sampling port, intake and exhaust manifolds respectively [11].

The rate of EGR is

$$\mathrm{EGR}=\frac{\dot m_{\mathrm{EGR}}}{\dot m_{\mathrm{mix}}}=\frac{\dot m_{\mathrm{EGR}}}{\dot m_{\mathrm{EGR}}+\dot m_{\mathrm{air}}+\dot m_{\mathrm{fuel}}}=\frac{1}{1+\frac{\dot m_{\mathrm{fuel}}}{\dot m_{\mathrm{EGR}}}+\frac{\dot m_{\mathrm{air}}}{\dot m_{\mathrm{EGR}}}}=\frac{1}{1+\frac{1}{\dot m_{\mathrm{EGR}}}*\left(\dot m_{\mathrm{air}}+\dot m_{\mathrm{fuel}}\right)} \tag{1}$$

where $\dot m_{\mathrm{mix}}$ represents the mass balance of the intake mixture of gases. The mass flow of CO_2 for each intake mixture component is determinate by a mass balance:

$$\dot m_{\mathrm{CO_{2mix}}}=\dot m_{\mathrm{CO_{2EGR}}}+\dot m_{\mathrm{CO_{2air}}}+\dot m_{\mathrm{CO_{2fuel}}} \tag{2}$$

as there is no reaction for the CO_2:

$$\dot N_{\mathrm{CO_{2mix}}}=\dot N_{\mathrm{CO_{2EGR}}}+\dot N_{\mathrm{CO_{2air}}}+\dot N_{\mathrm{CO_{2fuel}}} \tag{3}$$

the CO_2 molar fraction on the mix is:

$$Y_{\mathrm{CO_2,mix}}=\frac{\dot N_{\mathrm{CO_{2EGR}}}+\dot N_{\mathrm{CO_{2air}}}+\dot N_{\mathrm{CO_{2fuel}}}}{\dot N_{\mathrm{CO_{2mix}}}}=\frac{\dot N_{\mathrm{CO_{2EGR}}}+\dot N_{\mathrm{CO_{2air}}}+\dot N_{\mathrm{CO_{2fuel}}}}{\dot N_{\mathrm{air}}+\dot N_{\mathrm{fuel}}+\dot N_{\mathrm{EGR}}} \tag{4}$$

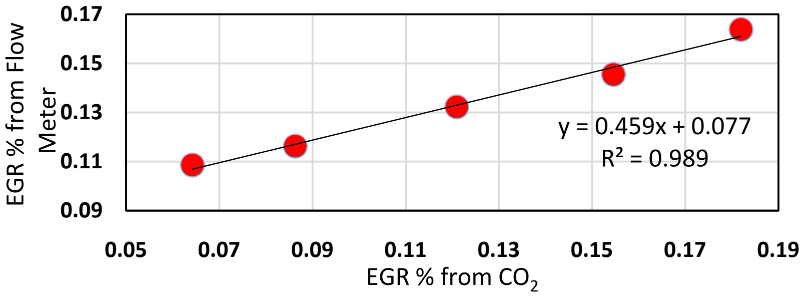

Figure 8. EGR flow calibration, CO_2 mass balance vs orifice flow meter measurement.

Knowing that $Y_{CO_2} = \dfrac{\dot{N}_{CO_2}}{\dot{N}}$ and $\dot{m} = \dot{N} * M$,

$$\begin{aligned} Y_{CO_2,\text{mix}} &= \frac{Y_{CO_{2EGR}} * \dot{N}_{\text{EGR}} + Y_{CO_{2air}} * \dot{N}_{\text{air}} + Y_{CO_{2fuel}} * \dot{N}_{\text{fuel}}}{\dot{N}_{CO_{2mix}}} \\ &= \frac{\dfrac{Y_{CO_{2EGR}} * \dot{m}_{\text{EGR}}}{M_{\text{EGR}}} + \dfrac{Y_{CO_{2air}} * \dot{m}_{\text{air}}}{M_{\text{air}}} + \dfrac{Y_{CO_{2fuel}} * \dot{m}_{\text{fuel}}}{M_{\text{fuel}}}}{\dfrac{\dot{m}_{\text{mix}}}{M_{\text{mix}}}} \\ &= \frac{\dfrac{Y_{CO_{2fuel}} * \dot{m}_{\text{EGR}}}{M_{\text{EGR}}} + \dfrac{Y_{CO_{2air}} * \dot{m}_{\text{air}}}{M_{\text{air}}} + \dfrac{Y_{CO_{2fuel}} * \dot{m}_{\text{fuel}}}{M_{\text{fuel}}}}{\dfrac{\dot{m}_{CO_{2EGR}} + \dot{m}_{CO_{2air}} + \dot{m}_{CO_{2fuel}}}{M_{\text{mix}}}} \end{aligned} \tag{5}$$

Equations (1) and (5) contain 2 unknowns, EGR and $\dot{m}_{\text{EGR}}$. Solving for $\dot{m}_{\text{EGR}}$ in Equation (5) and substituting on Equation (1):

$$\dot{m}_{\text{egr}} = \frac{\dfrac{Y_{CO_{2fuel}} * \dot{m}_{\text{fuel}}}{M_{\text{fuel}}} + \dfrac{Y_{CO_{2air}} * \dot{m}_{\text{air}}}{M_{\text{air}}} - \dfrac{Y_{CO_{2mix}} * \left(\dot{m}_{\text{fuel}} + \dot{m}_{\text{air}}\right)}{M_{\text{mix}}}}{\dfrac{Y_{CO_{2mix}}}{M_{\text{mix}}} - \dfrac{Y_{CO_{2egr}}}{M_{\text{egr}}}} \tag{6}$$

Knowing the mass flow of EGR gases, the EGR rate is calculated from Equation (1).

3. Baseline Testing

The baseline testing defines the initial performance condition of the SCE and helps to compare with the available commercial natural gas engine offered by Cummins (6-cylinder 12-liter NG engine). The baseline consisted of two sections: preliminary engine development and baseline efficiency.

The EGR effect on efficiency and the best thermal efficiency with baseline hardware configuration was evaluated for the SCE. Using fixed EGR rate values, a CA50 timing sweep was carried out to find the best efficiency ignition timing. EGR rates from 5% to 20% were tested using fixed CA50, 16 bar IMEP, 50˚C intake temperature, and 1200 RPM. The results obtained are presented in **Figures 9-12**. For the cases of less EGR substitution, lower values of CA50 cases were not evaluated due to evident engine knock.

Maximum values of brake power occur as CA50 is varied. The highest value is observed at 10% EGR. Larger timing values related to later CA50 show a pronounced decrease in power for every EGR rate because heat release timing is suboptimal, occurring too late. The best thermal efficiency (39.9%) is at the 10% EGR and earliest knock-free CA50 value (8 deg ATDC). Additionally, all the cases evaluated achieved values above 39% BTE. Two cases of mid-EGR rate and 8 deg CA50 show lower values that disrupt the trend. These peak efficiency values are within the expected ranges for this engine and the hardware configuration, with a BTE that is 2% lower than the result presented in other optimized

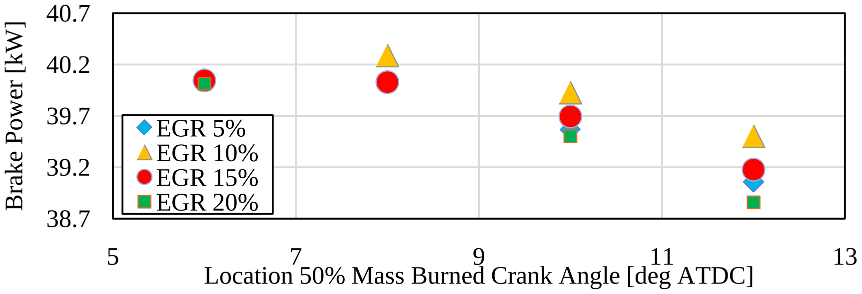

Figure 9. Location 50% mass burned crank angle vs brake power for different EGR ratios. Operation conditions 1200 RPM, target IMEP 16 bar.

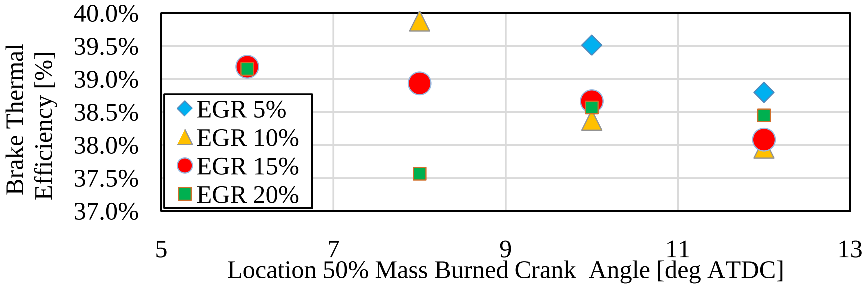

Figure 10. Location 50% mass burned crank angle vs brake thermal efficiency for different EGR ratios. Operation conditions 1200 RPM, IMEP 16 bar.

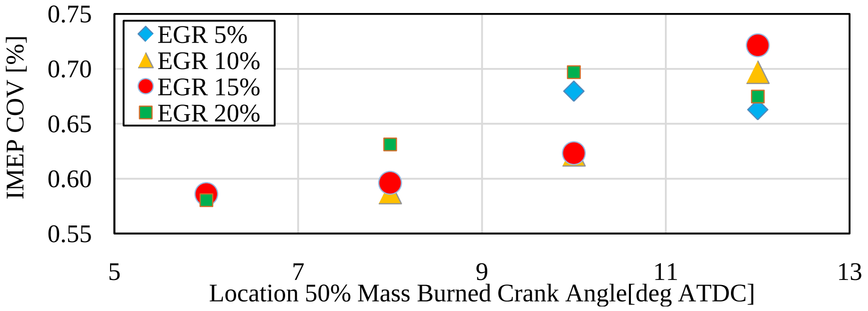

Figure 11. Location 50% mass burned crank angle vs peak pressure COV and IMEP COV for different EGR ratios. Operation conditions 1200 RPM, IMEP 16 bar.

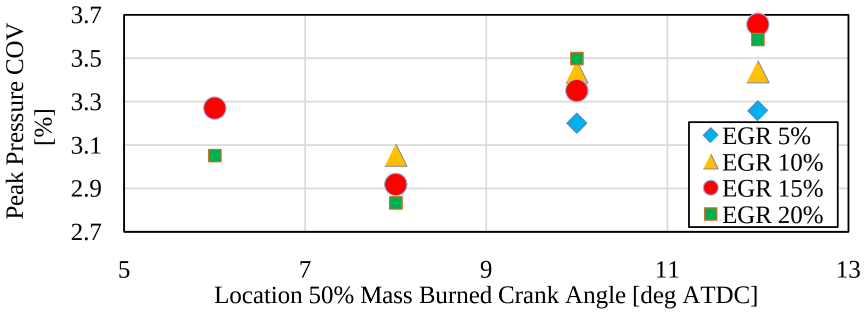

Figure 12. Location 50% mass burned crank angle vs COV and IMEP COV for different EGR ratios. Operation conditions 1200 RPM, IMEP 16 bar.

heavy-duty NG engines [12] [13]. Is important to mention that for the base line results presented, the engine was operated without using the innovative combustion control techniques and high EGR substitution rates that would allow improvements to combustion efficiency to achieve the final goal of this research of 44% BTE [8]. The peak pressure coefficient of variance (COV) is minimized at 8 deg CA50 for every condition tested (**Figure 11**). IMEP COV is below 1% for every condition tested and overall follows an inverse trend of the BTE and brake power (**Figure 12**). For both COV metrics, the lowest values are presented at the higher BTE conditions. For all the cases tested, the COV metrics indicate combustion stability below the threshold values of 3% and 10% respectively [10].

Combustion duration is characterized by the 0% to 10%, and the 10% to 90% mass fraction burned duration in crank angle degrees shown in **Figure 13** and **Figure 14**. The first one indicates the ignition delay or the time that it takes for the initiation of the combustion process. In this case, it takes a short period from 1 to 7 deg to reach 10% of the mass burned. The ignition delay decreases as the value of CA50 is decreased (advanced). Combustion duration, or 10% - 90% mass fraction burned, follows the same trend varying from 10 to 17 deg. Trends in heat release and cylinder pressure are directly related to the ignition timing. As spark timing is advanced the combustion occurs earlier with higher peak pressure. Faster combustion events show the higher BTE and brake power.

Combustion intensity (CI) metric was used to prevent the engine from entering into the knocking phase while allowing for higher BTE. In this case, specific testing was performing using CI as a control variable for the ignition instead of the mass burned percentage location. The lowest value of CI tested is 10% showing

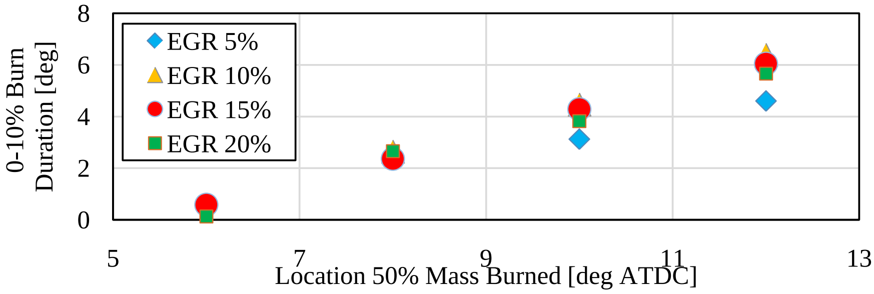

Figure 13. Location 50% mass burned crank angle vs 0% - 10% Burn Duration. Operation conditions 1200 RPM, IMEP 16 bar.

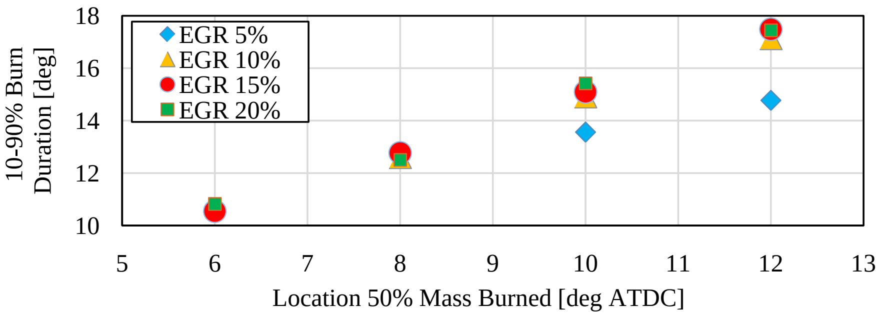

Figure 14. Location 50% Mass burned crank angle vs 10% - 90% Mass Burned. Operation conditions 1200 RPM, IMEP 16 bar.

the lowest BTE decreases and combustion instability and misfire are present for lower values. The highest value of CI required to operate the engine without approaching the medium and high knocking range is 40%. The BTE and Brake torque follow the same pattern as higher CI gives the best values for both metrics (**Figure 15**).

Figure 16 presents the efficiency map contour with respect to BMEP and rate of EGR. Best BTE is found on the upper line at higher BMEP and 8% EGR rate. Subsequent lines show bell shaped decreasing behavior of the BTE, pointing a higher BTE area around 12% rate EGR. A similar contour with respect to ignition timing variation where the best efficiency region is located at 8 deg ATDC for the location of 50% mass burned, with a range of BMEP from 15.7 to 16.3 bar. The base line testing intended to identify the knock limits of the engine with the particular hardware configuration selected.

Crank resolute data is used to analyze the combustion characteristics. **Figure 17** presents the effect of EGR substitution rate over in cylinder pressure and normalized apparent heat release rate. Keeping constant ignition timing target, CA50 10 deg ATDC and IMEP 16 bar, the highest peak pressure and steepest

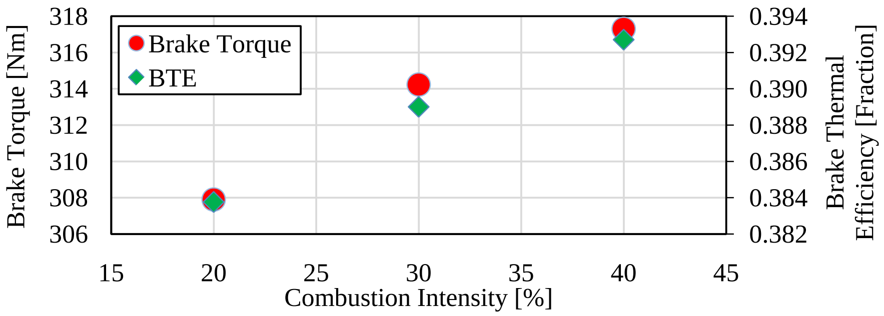

Figure 15. Combustion Intensity vs Brake Torque and Brake Thermal Efficiency. Operation conditions IMEP 16 bar, EGR 20%.

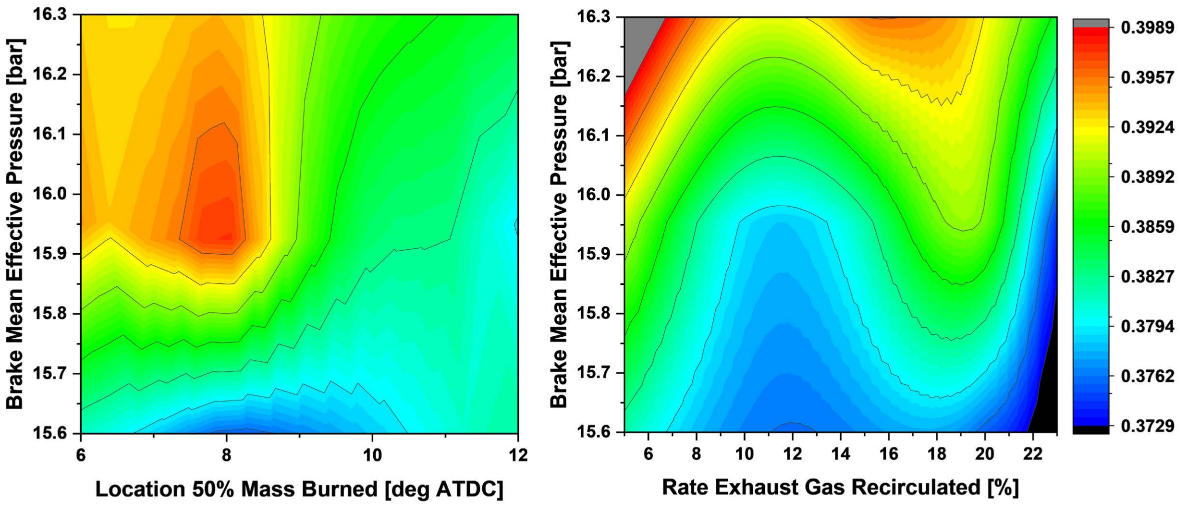

Figure 16. Efficiency map showing contours of constant BTE with respect to Left: Rate of EGR [%] and BMEP [bar]; Right: Location 50% Mass Burned [deg ATDC] and Brake Mean Effective Pressure [bar].

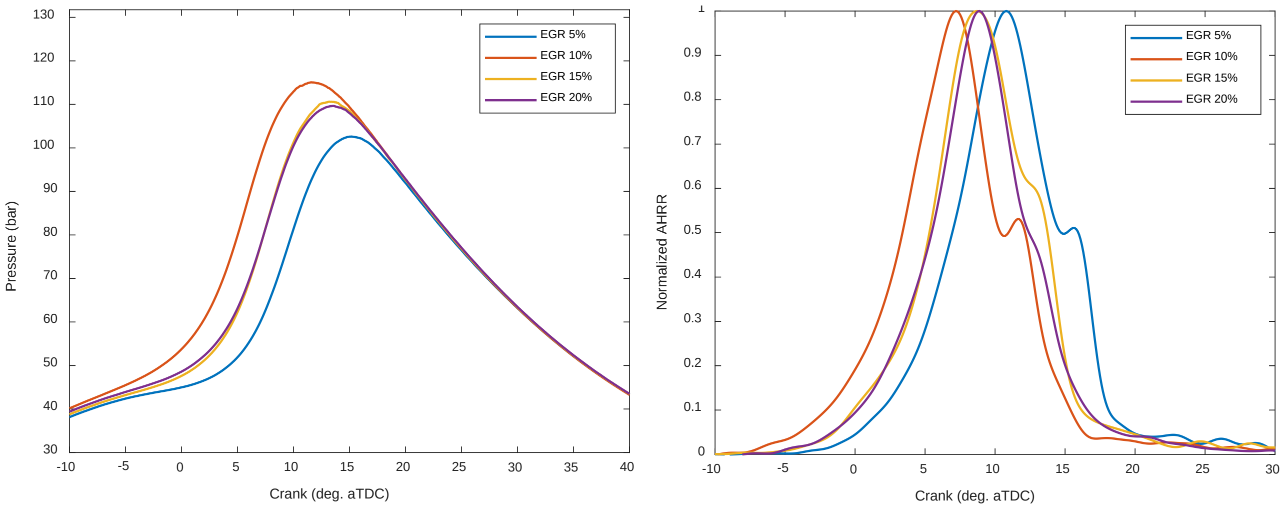

Figure 17. Effect of EGR substitution rate: Left: crank angle degree after TDC vs mean in-cylinder pressure trace [bar]; Right: crank angle degree after TDC vs normalized accumulated heat release.

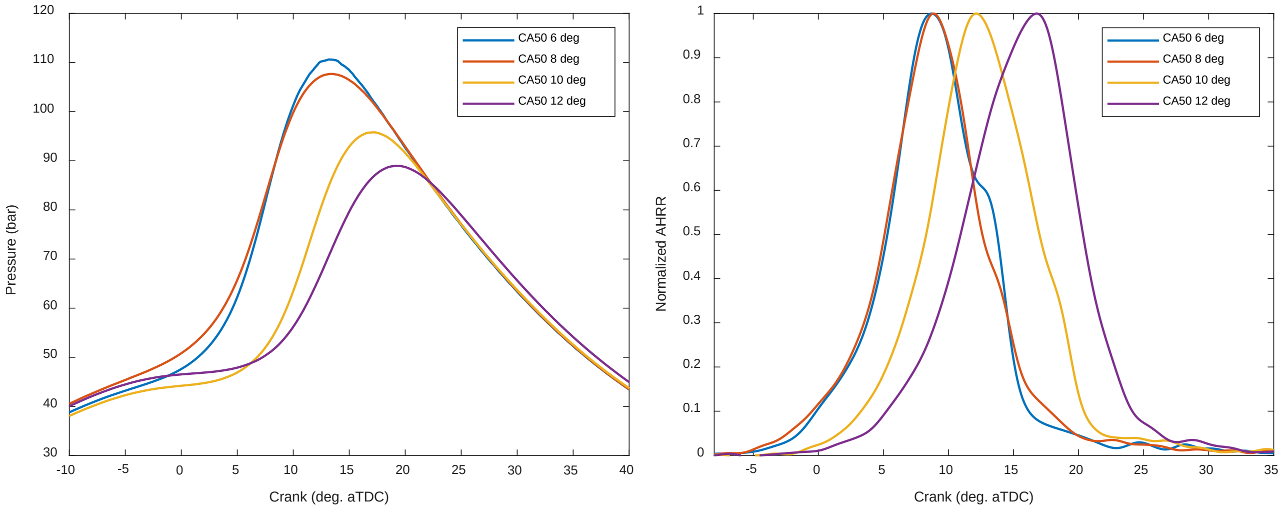

Figure 18. Effect of ignition timing, location 50% mass burned (CA50): Left: crank angle degree after TDC vs mean in-cylinder pressure trace [bar]; Right: crank angle degree After TDC vs normalized accumulated heat release.

pressure increase is for the most efficient BTE case, 10% EGR, while the lowest case is for the least EGR substitution 5%. No clear difference is encountered for the highest EGR substitution 15% and 20%. With respect to the Normalized Apparent Heat Release Rate (AHRR), the same trend is present whit faster and earlier combustion for the most efficient case (EGR 10%). Important to note the shoulder on the last part of the heat release for this case, which indicates the presence of a second combustion event, that is considered End Gas Autoignition (EGAI) [14].

Figure 18 shows the effect of ignition timing in terms of location of CA50 for the same EGR substitution rate 15% and IMEP 16 bar. The pressure trace divides in two couples with earliest CA50 showing very similar results and a close relationship for the cases of 10 and 12 deg ATDC CA50. As expected the highest

BTE is present with the earliest ignition timing, explained by the behavior of the AHRR that has the steepest trace heat release and the same combustion duration, with only a minor difference indicating the presence of a second heat release (combustion event under EGAI conditions) for the 6 deg ATDC case. The 10 and 12 deg ATDC cases decrease on the slope and show how the energy from the fuel is released later on the crank rotation.

4. Conclusions

Effective control of intake manifold pressure, exhaust manifold pressure, engine equivalence ratio, speed, torque, jacket water temperature, and oil temperature have been demonstrated. The baseline testing shows reliable and consistent results for engine thermal efficiency indicated mean effective pressure (IMEP), and coefficient of variance of the IMEP over a wide range of operating conditions.

- The engine was operated with load ranges from 15.5 to 16.4 bar IMEP at 1200 RPM with a best thermal efficiency of 39.9% at 10% EGR substitution rate and a CA50 value of 8 deg ATDC. The achieved BTE for this engine was expected for the baseline hardware configuration tested, with peak values 2% lower than similar heavy duty NG engines while operating with lower EGR rate substitution rates;
- The knock limit for the engine was encountered at 6 deg ATDC CA50 for the cases with 15% and 20 EGR substitution rate, and 16.4 bar and for 15% and 20% EGR. The capability to achieve over 30% EGR substitution rates was demonstrated;
- The COV of IMEP was below 1% for all the test cases while the COV of Peak Pressure was below 3.7% for all the cases tested, showing combustion stability lower than threshold values of 3% and 10% respectively;

This test cell will be used to conduct a research program to develop new and innovative control algorithms and CFD optimized combustion chamber designs, allowing ultra-high efficiency and low emissions for NG ICE's heavy-duty on-road applications.

Acknowledgements

The work presented on this paper was funded by the Department of Energy through the Office of Energy Efficiency and Renewable Energy under grant number DE-EE0008331. Fulbright Scholarship "Fulbright Colombia—PALC", founded author JFR. The authors would like to thank our project partners, Cummins Inc. and Woodward, Inc. for their valuable contributions.

Conflicts of Interest

The authors declare no conflicts of interest regarding the publication of this paper.

References

[1] Liu, J. and Dumitrescu, C.E. (2020) Limitations of Natural Gas Lean Burn Spark Ig-

nition Engines Derived from Compression Ignition Engines. *Journal of Energy Resources Technology*, **142**, Article ID: 122308. https://doi.org/10.1115/1.4047404

[2] Kalghatgi, G. (2014) The Outlook for Fuels for Internal Combustion Engines. *International Journal of Engine Research*, **15**, 383-398. https://doi.org/10.1177/1468087414526189

[3] Heywood, J. (1998) Internal Combustion Engine Fundamentals. McGraw-Hill, New York.

[4] Dumitrescu C.E., Padmanaban, V. and Liu, J.L. (2018) An Experimental Investigation of Early Flame Development in an Optical SI Engine Fueled with Natural Gas. *Journal of Engineering for Gas Turbines and Power*, **140**, Article ID: 082802. https://doi.org/10.1115/1.4039616

[5] Olsen, D.B. and Mitchell, R.H. (2018) Extending Substitution Limits of a Diesel-Natural Gas Dual Fuel Engine. *Journal of Energy Resources Technology*, **140**, Article ID: 052202. https://doi.org/10.1115/1.4038625

[6] Mohr, J., Zdanowicz, A., Tryner, J., Gustafson, K., Venegas, J., Windom, B., Olsen, D. and Marchese, A. (2019) Ignition, Flame Propagation, and End-Gas Autoignition Studies of Natural Gas/EGR Blends in a Rapid Compression Machine. 2019 *WSSCI Fall Technical Meeting*, Albuquerque, New Mexico, 14-15 October 2019.

[7] Bestel, D., Windom, B., Olsen, D., Marchese, A., Bayliff, S. and Xu, H. (2019) 3-D Modeling of the CFR Engine for the Investigation of Knock on Natural Gas. 2019 *Fall Meeting of the Western States Section of the Combustion Institute*, Albuquerque, New Mexico, 14-15 October 2019.

[8] Bayliff, S., Marchese, A., Windom, B. and Olsen, D. (2019) The Effect of EGR on Knock Suppression, Efficiency, and Emissions in a Stoichiometric, Spark Ignited, Natural Gas Engine. 2019 *WSSCI Fall Technical Meeting*, Albuquerque, New Mexico, 14-15 October 2019.

[9] Bayliff, S. (2020) Evaluation of Controlled End Gas Auto Ignition with Exhaust Gas Recirculation in a Stoichiometric, Spark Ignited, Natural Gas Engine. Colorado State University, Fort Collins, CO, USA. https://doi.org/10.1115/1.0003702V

[10] Kirkpatrick, A.T. (2020) Internal Combustion Engines: Applied Thermosciences. Wiley, Hoboken. https://doi.org/10.1002/9781119454564

[11] Turns, S.R. (2012) An Introduction To Combustion Concepts and Applications. McGraw Hill, New York.

[12] Kaiadi, M., Tunestal, P. and Johansson, B. (2010) Improving Efficiency, Extending the Maximum Load Limit and Characterizing the Control-Related Problems Associated with Higher Loads in a 6-Cylinder Heavy-Duty Natural Gas Engine. *ASME Internal Combustion Engine Division* 2010 *Fall Technical Conference*, San Antonio, 12-15 September, 885-892. https://doi.org/10.1115/ICEF2010-35012

[13] Kocsis, M., Mitchell, R., Mois, A.A., Kalaskar, V., Sjovall, S. and William, R. (2020) Improving Heavy Duty Natural Gas Engine Efficiency: A Systematic Approach to Application of Dedicated EGR. *WCX SAE World Congress Experience*, Detroit Michigan, United States, 21-23 April 2020. https://doi.org/10.4271/2020-01-0818

[14] Bestel, D., Rodriguez, J., Marchese, A., Olsen, D. and Windom, B. (2022) Detection and Onset Determination of End-Gas Autoignition on Spark-Ignited Natural Gas Engines Based on the Apparent Heat Release Rate. *WCX SAE World Congress Experience,* Detroit, 5-7 April.